Chapter 7

Lattice vibrations

7.1 Introduction

Up to this point in the lecture, the crystal lattice was always assumed to be completely rigid, i.e. atomic displacements away from the positions of a perfect lattice were not considered. For this case, we have developed a formalism to compute the electronic ground state for an arbitrary periodic atomic configuration and therewith the total energy of our system. Although it is obvious that the assumption of a completely rigid lattice does not make a lot of sense (it even violates the uncertainty principle), we obtained with it a very good description for a wide range of solid state properties, among which were the electronic structure (band structure), the nature and strength of the chemical bonding, or low temperature cohesive properties like the stable crystal lattice. The reason for this success is that the internal energy U of the solid (or similarly of a molecule) can be written as

$$U = E^{\text{static}} + E^{\text{vib}} \quad , \tag{7.1}$$

where E^{static} is the electronic ground state energy with a fixed lattice (on which we have focused so far) and E^{vib} is the additional energy due to lattice motion. In general (and we will substantiate this below), $E^{\text{static}} \gg E^{\text{vib}}$ and thus many properties are correctly obtained, even when simply neglecting E^{vib}.
There is, however, also a multitude of solid state properties, for which the consideration of lattice mobility is crucial. Mobility is in this respect already quite a big word, because for many of these properties it is enough to take small vibrations of the ions around their (ideal) equilibrium position into account. And although the amplitude of these vibrations is small, the important aspect about them is that they can describe deformations whose wavelength is comparable to the interatomic distances – which is thus outside of the validity of continuum elasticity theory. The vibrational modes of crystalline lattices are called *phonons*, and most salient examples of solid state properties for which they are of paramount importance are:

- **Heat capacity:** In metals with a rigid perfect lattice, only the free electron like conduction electrons can take up small amounts of energy (of the order of thermal energies). The specific heat capacity due to these conduction electrons was computed to vary linearly with temperature for $T \to 0$ in the first exercise. In insulators with the same rigid perfect lattice assumption, not even these degrees of freedom are available. Correspondingly, the only excitations would be electronic excitations across the (huge) band gap $E_g \gg k_B T$. Their (vanishingly small) probability will be $\sim \exp(-E_g/k_B T)$, and the specific heat

would show a similar scaling at low temperatures accordingly. In reality, one observes, however, that for both insulators and metals the specific heat varies predominantly with T^3 at low temperatures, in clear contradiction to the above cited rigid lattice dependencies.

- **Thermal expansion:** Due to the negligibly small probability of electronic excitations over the gap, there is nothing left in a rigid lattice insulator that could account for the pronounced thermal expansions typically observed in experiments. These expansions are, on the other hand, key to many engineering applications of materials sciences (different pieces simply have to fit together over varying temperatures). Likewise, for structural phase transitions upon heating and finally melting the static lattice approximation fails with a vengeance.

- **Transport properties:** In a perfectly periodic potential Bloch electrons suffer no collisions (being solutions to the many-body Hamiltonian). Assuming only point defects as responsible for finite path lengths, one can not explain quantitatively the really measured, and obviously *finite* electric and thermal conductance of metals and semiconductors. Scattering of electrons, propagation of sound, heat transport, or optical absorption are all fundamental properties of real devices (like transistors, LED's, lasers). They are among other things responsible for the electric resistance and loss of the latter, and can only be understood when considering lattice vibrations.

7.2 Vibrations of a classical lattice

7.2.1 Adiabatic (Born-Oppenheimer) approximation

Throughout this chapter we assume that the electrons follow the atoms instantaneously, i.e. the kinetics of the electrons has no effect on the motion of the atoms. There is in particular no "memory effect" stored in the electronic motion (e.g. due to the electron cloud lacking behind the atomic motion). This is nothing else but the Born-Oppenheimer approximation, which we discussed at length in the first chapter. Within this approximation the potential energy (or Born-Oppenheimer) surface (PES) results from the electronic ground state for any given atomic structure (described by atomic positions $\{\mathbf{R}_I\}$, $I \in$ ion)

$$V^{\mathrm{BO}}(\{\mathbf{R}_I\}) \;=\; \min_{\Psi} E(\{\mathbf{R}_I\};\Psi) \quad . \tag{7.2}$$

The motion of the atoms/ions is then governed by the Hamiltonian

$$H \;=\; T^{\mathrm{ion}} \;+\; V^{\mathrm{BO}}(\{\mathbf{R}_I\}) \quad , \tag{7.3}$$

which does not contain the electronic degrees of freedom explicitly anymore. The complete interaction with the electrons (i.e. the chemical bonding) is instead contained implicitly in the form of the PES $V^{\mathrm{BO}}(\{\mathbf{R}_I\})$.
For a perfect crystal, the minima of this PES correspond to the points of a Bravais lattice (or better: to its basis) $\{\mathbf{R}_I^\circ\}$. And it was the situation with the atoms fixed exactly at $\{\mathbf{R}_I^\circ\}$, which we discussed exclusively in the preceding chapters in the rigid lattice model. There is, however, nothing that would confine the validity of the Born-Oppenheimer approximation to just the minima, or at least (recalling the discussion of the first chapter) the Born-Oppenheimer approximation will be equally good or bad for the minima and for the PES vicinity around them.

Correspondingly, understanding the properties of a crystal with the atoms at arbitrary positions $\{\mathbf{R}_I\}$ boils in the adiabatic approximation equally down to evaluating the PES at these positions. However, as long as the solid is not yet molten, we don't even need really arbitrary $\{\mathbf{R}_I\}$, but only ones that are very close to the (pronounced) minima corresponding to the ideal lattice. This allows us to write

$$\mathbf{R}_I \;=\; \mathbf{R}_I^\circ \;+\; \mathbf{s}_I \quad \text{with} \quad |\mathbf{s}_I| \ll a \qquad (a\text{: lattice constant}) \quad . \tag{7.4}$$

For such small displacements around a minimum, the PES can be approximated by a parabola and leads us to the *harmonic approximation*.

7.2.2 Harmonic approximation

For a classical, vibrating system the harmonic approximation corresponds to considering only vibrations with small amplitude. For such small amplitudes, the potential, in which the particle (or the particles) is/are moving, can be expanded in a Taylor series around the equilibrium geometry, keeping only the first leading term. To illustrate this, consider the classic example of the one-dimensional harmonic oscillator. The general Taylor expansion around a minimum at x_0 yields

$$V(x) \;=\; V(x_0) + \left[\frac{\partial}{\partial x}V(x)\right]_{x_0} s + \frac{1}{2}\left[\frac{\partial^2}{\partial x^2}V(x)\right]_{x_0} s^2 + \frac{1}{3!}\left[\frac{\partial^3}{\partial x^3}V(x)\right]_{x_0} s^3 + \ldots \quad , \tag{7.5}$$

with the displacement $s = x - x_0$. The linear term vanishes, because x_0 is an equilibrium geometry. For small displacements, the cubic (and higher) terms will be comparably small, leaving in the harmonic approximation only

$$V(x) \;\approx\; V(x_0) + \frac{1}{2}\left[\frac{\partial^2}{\partial x^2}V(x)\right]_{x_0} s^2 \quad . \tag{7.6}$$

Introducing the force acting on the particle

$$F \;=\; -\frac{\partial}{\partial x}V(x) \quad , \tag{7.7}$$

we see that the harmonic approximation (i.e. eq. (7.6)) corresponds to

$$F \;=\; -\frac{\partial}{\partial x}V(x) = -cs \quad , \tag{7.8}$$

where $c = \left[\frac{\partial^2}{\partial x^2}V(x)\right]_{x_0}$ is the spring constant. So, $V(x) = V(x_0) + \frac{c}{2}s^2$ results, i.e. we arrive at the potential of the harmonic oscillator.
A corresponding Taylor expansion can also be carried out in three dimensions for the Born-Oppenheimer surface, leading to

$$V^{\mathrm{BO}}(\mathbf{R}_1, \mathbf{R}_2, \ldots, \mathbf{R}_M) \;=\; V^{\mathrm{BO}}(\{\mathbf{R}_\mathrm{I}^\circ\}) \;+\; \frac{1}{2}\sum_{\substack{I=1,\\ J=1}}^{M,M}\sum_{\substack{\mu=1,\\ \nu=1}}^{3,3} s_{I,\mu}s_{J,\nu}\left[\frac{\partial^2}{\partial R_{I,\mu}\partial R_{J,\nu}}V^{\mathrm{BO}}(\{\mathbf{R}_I\})\right]_{\{\mathbf{R}_I^\circ\}} \quad , \tag{7.9}$$

where $\mu, \nu = x, y, z$ run over the three Cartesian coordinates, and the linear term has vanished again close to the equilibrium geometry. Defining the (3×3) matrix

$$\Phi_{\mu\nu}(\mathbf{R}_I, \mathbf{R}_J) \;=\; \left[\frac{\partial^2}{\partial R_{I,\mu} \partial R_{J,\nu}} V^{\mathrm{BO}}(\{\mathbf{R}_I\})\right]_{\{\mathbf{R}_I^\circ\}} \quad , \tag{7.10}$$

the Hamilton operator for the M ions of the solid (and the N electrons implicitly contained in V^{BO}) can then be written as

$$H \;=\; \sum_{I=1}^{M} \frac{p_I^2}{2M_{\mathrm{ion},I}} + V^{\mathrm{BO}}(\{\mathbf{R}_I^0\}) + \frac{1}{2} \sum_{\substack{I=1 \\ J=1}}^{M,M} \sum_{\substack{\mu=1 \\ \nu=1}}^{3,3} s_{I,\mu} \Phi_{\mu\nu}(\mathbf{R}_I, \mathbf{R}_J) s_{J,\nu} \quad , \tag{7.11}$$

where $M_{\mathrm{ion},I}$ is the mass of ion I.
In other words, to evaluate H we need the second derivative of the PES at the equilibrium geometry with respect to the $3M$ coordinates $s_{I,\mu}$. Analytically, this is very involved, since the Hellmann-Feynman theorem can not be applied here. Alternatively, one exploits the three-dimensional analog to eq. (7.8), i.e.

$$\Phi_{\mu\nu}(\{\mathbf{R}_I, \mathbf{R}_J\}) \;=\; F_{I,\mu}(\mathbf{R}_1^\circ, \ldots, \mathbf{R}_J^\circ + s_{J,\mu}, \ldots, \mathbf{R}_M^\circ)/s_{J,\mu} \quad . \tag{7.12}$$

This way, the second derivative can be obtained numerically, by simply displacing an atom slightly from its equilibrium position and monitoring the arising forces on this and all other atoms. From this force point of view, it also becomes clear that many elements of the second derivative matrix will vanish: a small displacement of atom I will only lead to non-negligible forces on the atoms in its immediate vicinity. Atoms further away will not notice the displacement, and hence the second derivative between these atoms J and the initially displaced atom I will be zero.

$$\Phi_{\mu\nu}(\mathbf{R}_I, \mathbf{R}_J) \;=\; 0 \quad \text{for} \quad |\mathbf{R}_I^\circ - \mathbf{R}_J^\circ| \gg a_0 \quad , \tag{7.13}$$

where a_0 is the lattice parameter. Very often, one even finds

$$\Phi_{\mu\nu}(\mathbf{R}_I, \mathbf{R}_J) \;\simeq\; 0 \quad \text{for} \quad |\mathbf{R}_I^\circ - \mathbf{R}_J^\circ| > 2a_0 \quad . \tag{7.14}$$

Despite these simplifications, this numerical procedure is at this stage still unfortunately intractable, because we would have to do it for each of the M atoms in the solid (i.e. a total of $3M$ times). With $M \sim 10^{23}$, this is unfeasible, and we need to exploit further properties of solids to reduce the problem. Obviously, just like in the case of the electronic structure problem a much more efficient use of the periodicity of the lattice must be made. This is, however, not done at the level of further specifying the total Hamilton operator, but in the equations of motion following from the general form of eq. (7.11).

7.2.3 Classical equations of motion

Before further analyzing the quantum mechanical problem, it is instructive to first discuss what follows out of the classical Hamilton function corresponding to eq. (7.11). We will see that the classical treatment emphasizes more the wave-like character of the lattice vibrations, whereas a particle (corpuscular) character follows from the quantum mechanical treatment. This is not new, but just another example of the wave-particle dualism known e.g. from light/photons.

In the classical case and knowing the structure of the Hamilton function from eq. (7.11), the total energy (as sum of kinetic and potential energy) can be written as

$$E = \sum_{I=1}^{M} \frac{M_{\mathrm{ion},I}}{2} \dot{\mathbf{s}}_I + V^{\mathrm{BO}}(\{\mathbf{R}_I^\circ\}) + \frac{1}{2} \sum_{\substack{I=1,\\J=1}}^{M,M} \sum_{\substack{\mu=1,\\\nu=1}}^{3,3} s_{I,\mu} \Phi_{\mu\nu}(\mathbf{R}_I, \mathbf{R}_J) s_{J,\nu} \tag{7.15}$$

The classical equation of motion of the nuclei in our system (within the harmonic approximation) can be written as

$$M_{\mathrm{ion},I}\, \ddot{s}_{I,\mu} = -\sum_{J,\nu} \Phi_{\mu\nu}(\mathbf{R}_I, \mathbf{R}_J) s_{J,\nu} \quad , \tag{7.16}$$

where the right hand side represents the μ-component of the force vector acting on atom I of mass $M_{\mathrm{ion},I}$ and the double dot above s represents the second time derivative. As a first step, we will get rid of the time dependence. A general form of solution for the second-order differential equation (eq. (7.16)) is

$$s_{I,\mu}(t) = u_{I,\mu} e^{i\omega t} \quad . \tag{7.17}$$

Inserting into eq. (7.16) leads to

$$M_{\mathrm{ion},I} \omega^2 u_{I,\mu} = \sum_{J,\nu} \Phi_{\mu\nu}(\mathbf{R}_I, \mathbf{R}_J) u_{J,\nu} \quad . \tag{7.18}$$

This is a system of coupled algebraic equations with $3M$ unknowns (still with $M \sim 10^{23}$!). As already remarked above, it is hence not directly tractable in this form, and we exploit (just like in the electronic case), that the solid has in its equilibrium geometry a periodic lattice structure. Correspondingly, we decompose the coordinate $\mathbf{R}_I$ into a Bravais vector $\mathbf{R}_n$ (pointing to the unit cell) and a vector $\mathbf{R}_\alpha$ pointing to atom α of the basis within the unit cell,

$$\mathbf{R}_I = \mathbf{R}_n + \mathbf{R}_\alpha \quad . \tag{7.19}$$

Formally, we can therefore replace the index I over all atoms in the solid by the index pair (n, α) running over the unit cells and different atoms in the basis. With this, the matrix of second derivatives takes the form

$$\Phi_{\mu\nu}(\mathbf{R}_I, \mathbf{R}_J) = \Phi_{\alpha\mu}^{\beta\nu}(n, n') \quad . \tag{7.20}$$

And in this form, we can now start to exploit the periodicity of the Bravais lattice. From the translational invariance of the lattice follows e.g. immediately that

$$\Phi_{\alpha\mu}^{\beta\nu}(n, n') = \Phi_{\alpha\mu}^{\beta\nu}(n - n') \quad . \tag{7.21}$$

From a classical point of view, $\{\mathbf{s}_I(t)\}$ is simply a snap shot of the displacement field of the atoms at time t. This suggests, that $\mathbf{u}_I$ may be describable by means of a vibration

$$u_{\alpha\mu}(\mathbf{R}_n) = \frac{1}{\sqrt{M_{\mathrm{ion},\alpha}}} c_{\alpha\mu} e^{i\mathbf{k}\mathbf{R}_n} \tag{7.22}$$

where c is the amplitude of displacement, or through a superposition of several different of such vibrations. Using this ansatz for eq. (7.18) we obtain

$$\omega^2 c_{\alpha\mu} = \sum_{\beta\nu} \left\{ \sum_{n'} \frac{1}{\sqrt{M_\alpha M_\beta}} \Phi_{\alpha\mu}^{\beta\nu}(n - n') e^{i\mathbf{k}(\mathbf{R}_n - \mathbf{R}_{n'})} \right\} c_{\beta\nu} \quad . \tag{7.23}$$

Note that the part in curly brackets is only formally still dependent on the position $\mathbf{R}_I$ (through the index n). Since all unit cells are equivalent, $\mathbf{R}_I$ is just an arbitrary zero for the summation over the whole Bravais lattice. This part in curly brackets

$$D^{\beta\nu}_{\alpha\mu}(\mathbf{k}) \;=\; \frac{1}{\sqrt{M_\alpha M_\beta}} \sum_{n'} \Phi^{\beta\nu}_{\alpha\mu}(n-n') e^{i\mathbf{k}(\mathbf{R}_n - \mathbf{R}_{n'})} \quad , \tag{7.24}$$

is called *dynamic matrix*, and its definition allows us to rewrite the homogeneous linear system of equations in a very compact way

$$\omega^2 c_{\alpha\mu} \;=\; \sum_{\beta\nu} D^{\beta\nu}_{\alpha\mu}(\mathbf{k}) c_{\beta\nu} \tag{7.25}$$

Compared to the original equation of motion, cf. eq. (7.18), a dramatic simplification has been reached: due to the lattice symmetry we achieved to reduce the system of $3r \times M$ equations to $3r$ equations, where r is the number of atoms in the basis of the unit cell. The price we paid for it is that we have to solve the equations of motion for each $\mathbf{k}$ anew. This is comparably easy, though, since this scales linearly with the number of $\mathbf{k}$ and not cubic like the matrix inversion, and has to be done only for few $\mathbf{k}$ (since we will see that the k-dependent functions are quite smooth). From eq. (7.25) one gets then as condition for the existence of solutions the eigenvalue problem (i.e. solutions must satisfy the following:)

$$\det\left(\hat{D}(\mathbf{k}) - \omega^2 \hat{1}\right) = 0 \quad . \tag{7.26}$$

This problem has $3r$ eigenvalues, which are functions of the wave vector $\mathbf{k}$,

$$\omega \;=\; \omega_i(\mathbf{k}) \quad , \quad i = 1, 2, \ldots, 3r \tag{7.27}$$

and to each of these eigenvalues $\omega_i(\mathbf{k})$, eq. (7.25) provides the eigenvector

$$c_{\alpha\mu} \;=\; e^{(i)}_{\alpha\mu}(\mathbf{k}) \qquad \text{viz.} \quad \mathbf{c}_\alpha \;=\; \mathbf{e}^{(i)}_\alpha(\mathbf{k}) \quad . \tag{7.28}$$

These eigenvectors are determined up to a constant factor, and this factor is finally obtained by requiring all eigenvectors to be normalized (and orthogonal to each other).
In conclusion, one then determines for the displacement $\mathbf{s}_{n\alpha}(t)$ of atom $I = (n, \alpha)$ away from the equilibrium position at time t

$$\mathbf{s}^{(i)}_{n\alpha}(t) \;=\; \frac{1}{\sqrt{M_{\text{ion},\alpha}}} \mathbf{e}^{(i)}_\alpha(\mathbf{k}) e^{i(\mathbf{k}\mathbf{R}_n - \omega_i(\mathbf{k})t)} \tag{7.29}$$

as a special solution to the equation of motion (7.16), i.e. the one corresponding to the particular normal mode $(\mathbf{k}, \omega(\mathbf{k}))$. With this, the system of $3M$ three-dimensional coupled oscillators is transformed into $3M$ decoupled (but "collective") oscillators, and the solutions (or so-called *normal modes*) correspond to waves, spreading over the whole crystal (i.e. these waves have only a formal resemblance to what we think of traditionally as an oscillator). Any arbitrary displacement situation of the atoms (i.e. the general solution) can now be written as an expansion in these special solutions, i.e. the waves form the basis for the description of lattice vibrations.

7.2.4 Comparison between $\varepsilon_n(\mathbf{k})$ und $\omega_i(\mathbf{k})$

We have derived the normal modes of lattice vibrations exploiting the periodicity of the ideal crystal lattice in a similar way as we did for the electron waves in chapters 4 and 5. Since it is only the symmetry that matters, the *dispersion relations* $\omega_i(\mathbf{k})$ will therefore exhibit a number of properties equivalent to those of the electronic eigenvalues $\varepsilon_n(\mathbf{k})$. We will not derive these general properties again, but simply list them here (check chapter 4 and 5 to see how they emerge from the periodic properties of the lattice):

1. $\omega_i(\mathbf{k})$ is periodic in k-space. The discussion can therefore always be restricted to the first Brillouin zone.

2. $\varepsilon_n(\mathbf{k})$ and $\omega_i(\mathbf{k})$ have the same symmetry within the Brillouin zone. Additionally to the space group symmetry of the lattice, there is also time inversion symmetry, yielding $\omega_i(\mathbf{k}) = \omega_i(-\mathbf{k})$.

3. Due to the use of periodic boundary conditions, the number of k-values is finite. When the solid is composed of M/r unit cells, then there are M/r different k-values in the Brillouin-zone. Since $i = 1 \ldots 3r$, there are in total $3r \times (M/r) = 3M$ values for $\omega_i(\mathbf{k})$, i.e. exactly the number of degrees of freedom of the crystal lattice.

4. $\omega_i(\mathbf{k})$ is an analytic function of $\mathbf{k}$ within the Brillouin zone. Whereas the band index n in $\varepsilon_n(\mathbf{k})$ can take arbitrarily many values, i in $\omega_i(\mathbf{k})$ is restricted to $3r$ values. We will see below that this is connected to the fact that electrons are fermions and lattice vibrations (phonons) bosons.

7.2.5 Simple one-dimensional examples

The difficulty of treating and understanding lattice vibrations is primarily one of book-keeping. The many indices present in the general formulae of section 7.2.2 and 7.2.3 let one easily forget the basic (and in principle simple) physics contained in them. It is therefore very useful (albeit academic) to consider toy model systems to *understand* the idea behind normal modes. The simplest possible system representing an infinite periodic lattice (i.e. with periodic boundary conditions) is a linear chain of atoms, and we will see that with the conceptual understanding obtained for one dimension it will be straightforward to generalize to real three-dimensional solids.

Linear chain with one atomic species

Consider an infinite one-dimensional linear chain of atoms of identical mass M, connected by springs with (constant) spring constant f as shown in Fig. 7.1. The distance between two atoms in their equilibrium position is a, and s_n the displacement of the nth atom from this equilibrium position. In analogy to eq. (7.16), the Newton equation of motion for this system is written as

$$M\,\ddot{s_n} = -f(s_n - s_{n+1}) + f(s_{n-1} - s_n) \quad , \tag{7.30}$$

i.e. the sum over all atoms breaks down to left and right nearest neighbor, and the second derivative of the PES corresponds simply to the spring constant. We solve this problem as

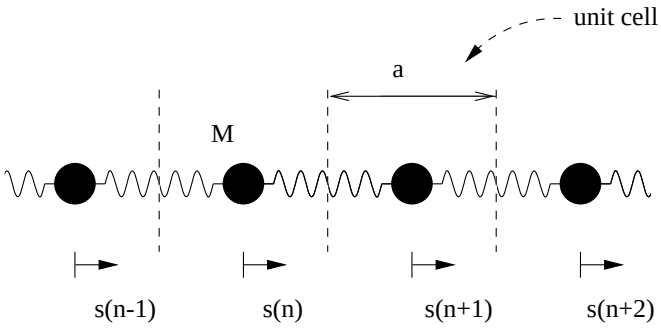

Figure 7.1: Linear chain with one atomic species (Mass M, and lattice constant a).

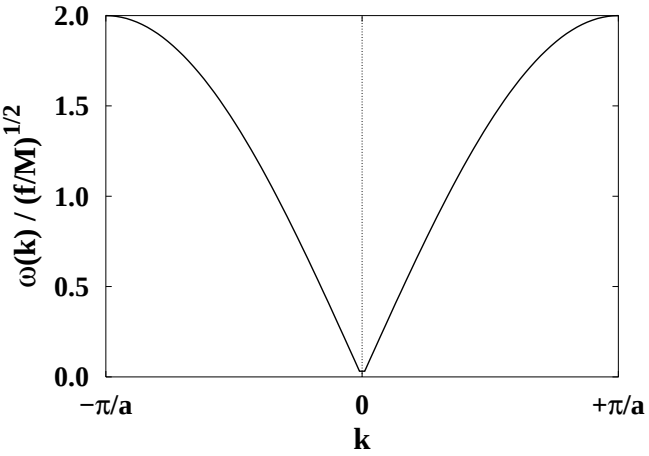

Figure 7.2: Dispersion relation $\omega(k)$ for the linear chain with one atomic species.

before by treating the displacement as a sinusoidally varying wave:

$$s_n = \frac{1}{\sqrt{M}} c e^{i(kan-\omega t)} \quad , \tag{7.31}$$

yielding

$$\omega^2 M = f\left(2 - e^{-ika} - e^{ika}\right) \quad . \tag{7.32}$$

Solving for ω, one therefore obtains

$$\omega(k) = 2\sqrt{\frac{f}{M}} \left|\sin\left(\frac{ka}{2}\right)\right| \quad , \tag{7.33}$$

i.e. as expected ω is a periodic function of k and symmetric with respect to k and $-k$. The first period lies between $k = -\pi/a$ and $k = +\pi/a$ (first Brillouin zone), and the form of the dispersion is plotted in Fig. 7.2. Equation (7.31) gives the explicit solutions for the displacement pattern in the linear chain for any wave vector k. They describe waves propagating along the chain with phase velocity ω/k and group velocity $v^g = \partial\omega/\partial k$.

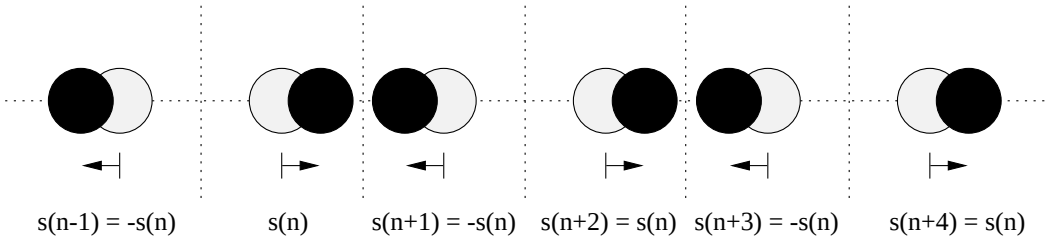

Figure 7.3: Snap shot of the displacement pattern in the linear chain at $k = +\pi/a$.

Let us look in more detail at the two limiting cases $k \to 0$ and $k \to \pi/a$ (i.e. the middle and border of the Brillouin zone). For $k \to 0$ we can approximate $\omega(k)$ given by eq. (7.33) with its leading term in the small k Taylor expansion ($\sin(x) \approx x$ for $x \to 0$)

$$\omega \approx \left(a\sqrt{\frac{f}{M}} \right) k \quad . \tag{7.34}$$

ω is thus linear in k, and the proportionality constant is simply the group velocity $v^g = a\sqrt{f/M}$, which is in turn identical to the phase velocity and independent of frequency. For the displacement pattern we obtain in this limit

$$s_n = \frac{1}{\sqrt{M}} c\, e^{ik(an - v^g t)} \quad , \tag{7.35}$$

i.e. at these small k-values (long wavelength) the phonons spread simply as vibrations with constant speed v^g (the ordinary sound speed in this 1D crystal!). This is the same result we would have equally obtained within linear elasticity theory, which is understandable because for such very long wavelength displacements the atomic structure and spacing is less important (the atoms move almost identically on a short length scale). Fundamentally, the existence of a branch of solutions whose frequency vanishes as k vanishes results from the symmetry requiring the energy of the crystal to remain unchanged, when all atoms are displaced by an identical amount. We will therefore always obtain such modes, regardless of whether we consider more complex interactions (e.g. spring constants to second nearest neighbors) or higher dimensions. Since their dispersion is close to the center of the Brillouin zone linear in k, which is characteristic of sound waves, these modes are commonly called *acoustic branches*.

One of the characteristic features of waves in discrete media, however, is that such a linear behaviour ceases to hold at wavelengths short enough to be comparable to the interparticle spacing. In the present case ω falls below $v^g k$ as k increases, the dispersion curve bends over and becomes flat (i.e. the group velocity drops to zero). At the border of the Brillouin zone (for $k = \pi/a$) we then obtain

$$s_n = \frac{1}{\sqrt{M}} c e^{i\pi n} e^{-i\omega t} \quad . \tag{7.36}$$

Note that $e^{i\pi n} = 1$ for even n, and $e^{i\pi n} = -1$ for odd n. This means that neighboring atoms vibrate against each other as shown in Fig. 7.3. This also explains, why in this case the highest frequency occurs. Again, the flattening of the dispersion relation is required by pure symmetry: From the repetition in the next Brillouin zone and with kinks forbidden, $\partial\omega/\partial k = 0$ must result at the Brillouin zone boundary, regardless of how much more complex and real we make our model.

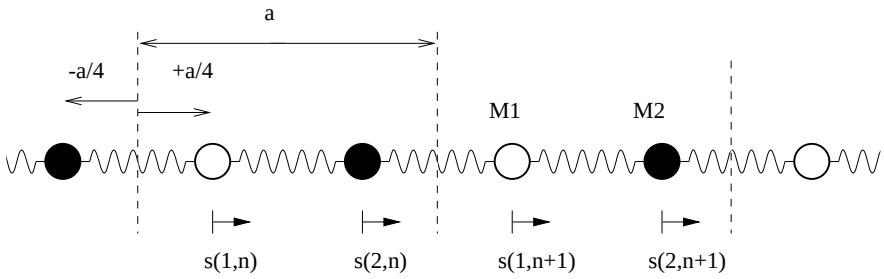

Figure 7.4: Linear chain with two atomic species (Masses $M1$ and $M2$). The lattice constant is a and the interatomic distance is $a/2$.

Linear chain with two atomic species

Next, we consider the case shown in Fig. 7.4, where there are two different atomic species in the linear chain, i.e. the basis in the unit cell is two. The equations of motion for the two atoms follow as a direct generalization of eq. (7.30)

$$M_1\,\ddot{s}_n^{(1)} = -f\left(s_n^{(1)} - s_n^{(2)} - s_{n-1}^{(2)}\right) \tag{7.37}$$

$$M_2\,\ddot{s}_n^{(2)} = -f\left(s_n^{(2)} - s_{n+1}^{(1)} - s_n^{(1)}\right) \quad . \tag{7.38}$$

Hence, also the same wave-like ansatz should work as before

$$s_n^{(1)} = \frac{1}{\sqrt{M_1}} c_1 e^{i\left(k(n-\frac{1}{4})a-\omega t\right)} \tag{7.39}$$

$$s_n^{(2)} = \frac{1}{\sqrt{M_2}} c_2 e^{i\left(k(n+\frac{1}{4})a-\omega t\right)} \quad . \tag{7.40}$$

This leads to

$$-\omega^2 c_1 = -\frac{2f}{\sqrt{M_1 M_2}} c_1 + \frac{2f}{\sqrt{M_1 M_2}} c_2 \cos\left(\frac{ka}{2}\right) \tag{7.41}$$

$$-\omega^2 c_2 = -\frac{2f}{\sqrt{M_1 M_2}} c_2 + \frac{2f}{\sqrt{M_1 M_2}} c_1 \cos\left(\frac{ka}{2}\right) \quad , \tag{7.42}$$

i.e. in this case the frequencies of the two atoms are still coupled to each other. The eigenvalues follow then from the determinant

$$\begin{vmatrix} \frac{2f}{\sqrt{M_1 M_2}} - \omega^2 & -\frac{2f}{\sqrt{M_1 M_2}} \cos\left(\frac{ka}{2}\right) \\ -\frac{2f}{\sqrt{M_1 M_2}} \cos\left(\frac{ka}{2}\right) & \frac{2f}{\sqrt{M_1 M_2}} - \omega^2 \end{vmatrix} = 0 \quad , \tag{7.43}$$

which yields the two solutions

$$\begin{aligned} \omega_\pm^2 &= f\left(\frac{1}{M_1} + \frac{1}{M_2}\right) \pm f\sqrt{\left(\frac{1}{M_1} + \frac{1}{M_2}\right)^2 - \frac{4}{M_1 M_2}\sin^2\left(\frac{ka}{2}\right)} \\ &= \frac{f}{\widetilde{M}} \pm f\sqrt{\frac{1}{\widetilde{M}^2} - \frac{4}{M_1 M_2}\sin^2\left(\frac{ka}{2}\right)} \quad , \end{aligned} \tag{7.44}$$

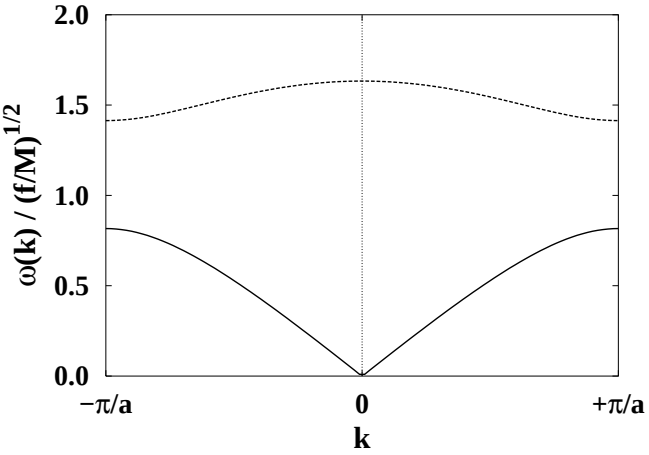

Figure 7.5: Dispersion relations $\omega(k)$ for the linear chain with two atomic species (the specific values are for $M_1 = 3M_2 = M$). Note the appearance of the optical branch not present in Fig. 7.2.

with the reduced mass $\widetilde{M} = \left(\frac{1}{M_1} + \frac{1}{M_2}\right)^{-1}$. We therefore obtain two branches for $\omega(k)$, the dispersion of which is shown in Fig. 7.5. As apparent, one branch goes to zero for $k \to 0$, $\omega_-(0) = 0$, as in the case of the monoatomic chain, i.e. we have again an *acoustic branch*. The other branch, on the other hand, exhibits interestingly a (high) finite value $\omega_+(0) = \sqrt{2\frac{f}{\widetilde{M}}}$ for $k \to 0$ and shows a much weaker dispersion over the Brillouin zone. Whereas in the acoustic branch both atoms within the unit cell move in concert, they vibrate against one another in opposite directions in the other solution. In ionic crystals (i.e. where there are opposite charges connected to the two species), these modes can therefore couple to electromagnetic radiation and are responsible for much of the characteristic optical behavior of such crystals. Correspondingly, they are generally (i.e. not only in ionic crystals) called *optical modes*, and their dispersion is called the *optical branch*.

At the border of the Brillouin zone at $k = \pi/a$ we finally obtain the values $\omega_+ = \sqrt{\frac{2f}{M_1}}$ and $\omega_- = \sqrt{\frac{2f}{M_2}}$, i.e. as apparent from Fig. 7.5 a gap has opened up between the acoustic and the optical branch. The width of this gap depends only on the mass difference of the two atoms (M_1 vs. M_2). For identical mass of the two species it closes, which is comprehensible, since then our model with equal spring constants *and* equal masses gets identical to the previously discussed model with one atomic species: the optical branch is then nothing but the upper half of the acoustic branch, folded back into the half-sized Brillouin zone.

7.2.6 Phonon band structure

With the conceptual understanding gained with the one-dimensional models, let us now proceed to look at the lattice vibrations of a real three-dimensional crystal. In principle, the formulae to describe the dispersion relations for the different solutions are already given in section 7.2.3. Most importantly, it is eq. (7.26) that gives us these dispersions (which are in their totality called *phonon band structure* in analogy to the electronic structure case). The crucial quantity is the

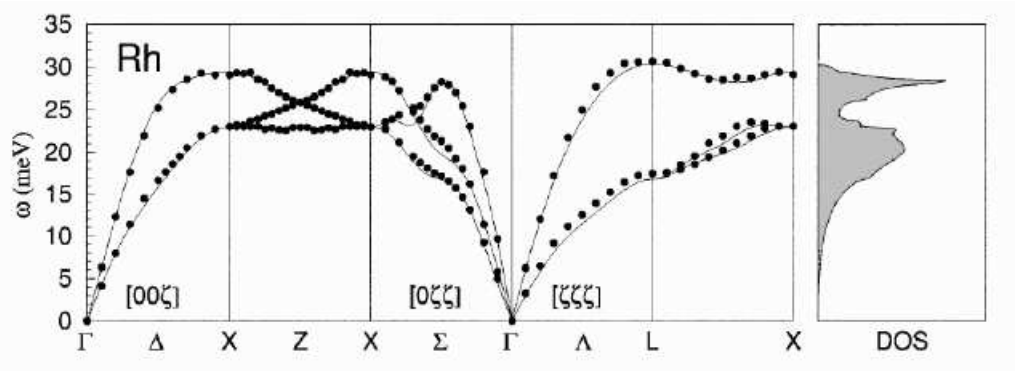

Figure 7.6: DFT-LDA and experimental phonon band structure (left) and corresponding density of states (right) for fcc bulk Rh [from R. Heid, K.-P. Bohnen and W. Reichardt, Physica B **263**, 432 (1999)].

dynamic matrix, and the different branches of the band structure follow from the eigenvalues after diagonalizing this matrix. This is also, what one computes in a quantitative approach to the phonon band structure problem, e.g. with density-functional theory. Since the dynamic matrix derives from the second derivatives of the total energy, one exploits for its computation in the so-called *direct (supercell) approach* (or frozen-phonon approach) the relation with the forces expressed in eq. (7.12). In other words, the different atoms in the unit cell are displaced by small amounts and the forces on all other atoms are recorded. In order to be able to compute the dynamic matrix with this procedure at different points in the Brillouin zone, larger supercells are employed and the (in principle equivalent) atoms within this larger periodicity displaced differently, so as to account for the different phase behavior. Obviously, this way only k-points that are commensurate to the used supercell periodicity can be accessed, and one runs into the problem that quite large supercells need to be computed in order to get the full dispersion curves. Approaches based on linear response (i.e. by inverting the dielectric matrix) are therefore also frequently employed. The details of the different methods go beyond the scope of the present lecture, but a good overview can for example be found in R.M. Martin, *Electronic Structure: Basic Theory and Practical Methods*, Cambridge University Press, Cambridge (2004). Experimentally, phonon dispersion curves are primarily measured using inelastic neutron scattering, and Ashcroft/Mermin dedicates an entire chapter to the particularities of such measurements. Overall, the measured and DFT-LDA/GGA calculated phonon band structures agree extremely well these days (regardless of whether computed by a direct or a linear response method), and instead of discussing the details of either measurement or calculation we rather proceed to some practical examples.

If one has a mono-atomic basis in the three-dimensional unit cell, we expect from the one-dimensional model studies that only acoustic branches should be present in the phonon band structure. There are, however, now 3 such branches, because in three-dimensions the orientation of the *polarization vector* (i.e. the eigenvector belonging to the eigenvalue $\omega(\mathbf{k})$), cf. eqs. (7.28) and (7.29) matters. In the linear chain, the displacement was only considered along the chain axis and such modes are called *longitudinal*. If the atoms vibrate in the three-dimensional case perpendicular to the propagation direction of the wave, two further *transverse modes* are obtained, and longitudinal and transverse modes must not necessarily exhibit the same disper-

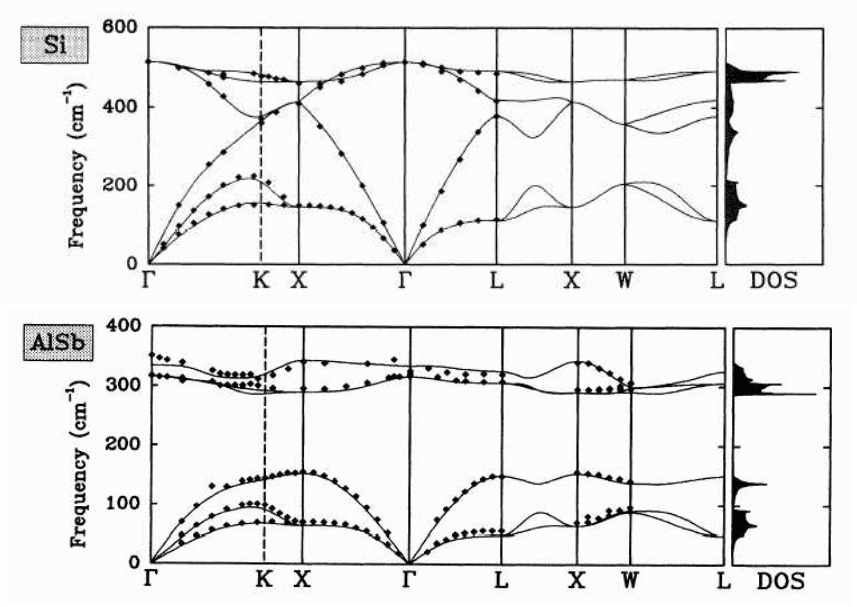

Figure 7.7: DFT-LDA and experimental phonon band structure (left) and corresponding density of states (right) for Si (upper panel) and AlSb (lower panel) in the diamond lattice. Note the opening up of the gap between acoustic and optical modes in the case of AlSb as a consequence of the large mass difference. 8 cm$^{-1} \approx 1$ meV [from P. Giannozzi *et al.*, Phys. Rev. B **43**, 7231 (1991)].

sion. Fig. 7.6 shows the phonon band structure for bulk Rh in the fcc structure, as well as the phonon density of states (DOS) resulting from it (which is obtained analogously to the electronic structure case by integrating over the Brillouin zone). The dispersion of the bands particularly along the lines $\Gamma - X$ and $\Gamma - L$, which run both from the Brillouin zone center to the border, has qualitatively the form discussed already for the linear chain model and is thus conceptually comprehensible.

Turning to a poly-atomic basis, the anticipated new feature is the emergence of optical branches due to vibrations of the different atoms against each other. This is indeed apparent in the phonon band structure of Si in the diamond lattice shown in Fig. 7.7, and we find for these branches again the rough shape that also emerged out of the di-atomic linear chain model (check again the $\Gamma - X$ and $\Gamma - L$ curves). Since there are in general $3r$ different branches for a basis of r atoms, cf. section 7.2.4, $3r - 3$ optical branches result (i.e. in the present case of a diatomic basis, there are 3 optical branches, one longitudinal one and two transverse ones). Although the diamond lattice has two inequivalent lattice sites (and represents thus a case with a di-atomic basis), these sites are both occupied by the same atom type in bulk Si. From the discussion of the di-atomic linear chain, we would therefore expect a vanishing gap between the upper end of the acoustic branches and the lower end of the optical ones. Comparing with Fig. 7.7 this is indeed the case. Looking at the phonon band structure of AlSb also shown in this figure, a huge gap can now, however, be discerned. This is obviously the result of the large mass difference between Al and Sb in this compound, and shows us that we can indeed understand most of the qualitative features of a real phonon band structure from the analysis of the two simple linear chain models. One should also have this inverse variation of the phonon frequencies with mass,

cf. eq. (7.24), in mind, in order to develop a rough feeling for the order of magnitude of lattice vibrational frequencies (or in turn the energies contained in these vibrations). For transition metals, cf. Fig. 7.6, we are talking about a range of 20-30 meV for the optical modes, while for lighter elements, cf. Fig. 7.7 this becomes increasingly higher. First row elements like oxygen in solids (thus oxides) exhibit optical vibrational modes around 70-80 meV, whereas the acoustic modes go in all cases down to zero at the center of the Brillouin zone. We are thus with all frequencies in the range of thermal energies, which already tells us how important these modes will be for the thermal behavior of the solid.

7.3 Quantum theory of the harmonic crystal

In the preceding section we have learnt to compute the lattice vibrational frequencies, when the ions are treated as classical particles. In practice, this approximation is not too bad for quite a range of materials properties. This has not only to do with that the mass of the ions is (with the exception of H and He) quite heavy, but also with that the quantum mechanical and the classical harmonic oscillator (on which all of the harmonic theory of lattice vibrations is based) exhibit many similar properties. In a very rough view, one can say that if only the vibrational frequency $\omega(\mathbf{k})$ of a mode itself is relevant, the classical treatment gives already a good answer (which is ultimately why we could understand the experimentally measured phonon band structure with our classical analysis). If, on the other hand, the energy connected with this mode $\omega(\mathbf{k})$ is important, or more precisely, the way how one excites (or populates) this mode is concerned, then the classical picture will fail. The prototypical example for this is the specific heat due to the lattice vibrations, which is nothing else but the measure of how effectively the vibrational modes of the lattice can take up thermal energy. In order to understand material properties of this kind, we need a quantum theory of the harmonic crystal. Just as in the classical case, let us first recall this theory for a one-dimensional harmonic oscillator before we really address the problem of the full solid state Hamiltonian.

7.3.1 One-dimensional quantum harmonic oscillator

Instead of just solving the quantum mechanical problem of the one-dimensional harmonic oscillator, the focus of this section will rather be to recap a specific formalism that can be easily generalized to the three-dimensional case of the coupled lattice vibrations afterwards. At first sight, this formalism might appear mathematically quite involved and seems to "overdo" for this simple problem, but in the end, the easy generalization will make it all worthwhile.
The classical Hamilton function for the one-dimensional harmonic oscillator is given by, cf. eq. (7.6),

$$H_{\mathrm{1D}}^{\mathrm{classic}} = T + V = \frac{p^2}{2m} + \frac{1}{2} f q^2 = \frac{p^2}{2m} + \frac{m\omega^2}{2} q^2 \quad , \tag{7.45}$$

where $f = m\omega^2$ is the spring constant and q the displacement. From here, the translation to quantum mechanics proceeds via the general rule to replace the momentum p by the operator

$$p = -i\hbar \frac{\partial}{\partial q} \quad , \tag{7.46}$$

where p and q satisfy the commutator relation

$$[p,q] = pq - qp = -i\hbar \quad , \tag{7.47}$$

which is in this case nothing but the Heisenberg uncertainty principle. The resulting Hamiltonian has then still the same form as in eq. (7.45), but p and q have now to be treated as (non-commuting) operators.
This structure can be considerably simplified by introducing the *lowering operator*

$$a = \sqrt{\frac{m\omega}{2\hbar}}\, q + i\sqrt{\frac{1}{2\hbar m\omega}}\, p \quad , \tag{7.48}$$

and the *raising operator*

$$a^\dagger = \sqrt{\frac{m\omega}{2\hbar}}\, q - i\sqrt{\frac{1}{2\hbar m\omega}}\, p \quad . \tag{7.49}$$

Note that the idea behind this pair of adjoint operators leads to the concept called second quantization, where a and $a^\dagger$ are denoted as *annihilation* and *creation operator*, respectively. The canonical commutation relation of eq. (7.47) implies then that

$$[a, a^\dagger] = 1 \quad , \tag{7.50}$$

and the Hamiltonian takes the simple form

$$H_{1\mathrm{D}}^{\mathrm{QM}} = \hbar\omega\left(a^\dagger a + \frac{1}{2}\right) \quad . \tag{7.51}$$

From this commutation relation and the form of the Hamiltonian it follows that the eigenstates $|n>$ ($n = 0, 1, 2, \ldots$) of this problem fulfill the relations (see any decent textbook on quantum mechanics for a derivation)

$$a^\dagger|n> = (n+1)^{1/2}\,|n+1> \tag{7.52}$$

$$a|n> = n^{1/2}\,|n-1> \qquad (n \neq 0) \tag{7.53}$$

$$a|0> = 0 \quad . \tag{7.54}$$

Application of the operator $a^\dagger$ brings the system therefore into one excited state higher, and application of the operator a one state lower. This explains the names given to these operators, in particular when considering that each excitation can be seen as one quantum. The creation operator creates therefore one quantum, while the annihilation operator wipes one out. With these recursion relations between the different states, the eigenvalues (i.e. the energy levels) of the one-dimensional harmonic oscillator are finally obtained as

$$E_n = < n|H_{1\mathrm{D}}^{\mathrm{QM}}|n> = (n+1/2)\hbar\omega \quad . \tag{7.55}$$

Note, that $E_0 \neq 0$, i.e. even in the ground state the oscillator has some energy (so-called energy due to *zero-point vibrations* or *zero-point energy*), whereas with each higher excited state one quantum $\hbar\omega$ is added to the energy. With the above mentioned picture of creation and annihilation operators, one therefore commonly talks about the state E_n of the system as corresponding to having excited n phonons of energy $\hbar\omega$. This nomenclature accounts thus for the discrete nature of the excitation and emphasizes more the corpuscular/particle view. In the classical case, the energy of the system was determined by the amplitude of the vibration and could take arbitrary continuous values. This is no longer possible for the quantum mechanical oscillator.

7.3.2 Three-dimensional quantum harmonic crystal

For the real three-dimensional system we will now proceed in an analogous fashion as in the simple one-dimensional case. To make the formulae not too complex, we will restrict ourselves in this section to the case of a mono-atomic basis (i.e. all ions have mass M_{ion} and $r = 1$). The generalization to poly-atomic bases is in principle then straightforward, but messes up the mathematics without yielding too much further insight.
In section 7.2.2 we had derived that the total Hamilton operator of the M ions in the harmonic approximation is given by

$$H = \sum_{I=1}^{M} \frac{p_I^2}{2M_{\text{ion}}} + V^{\text{BO}}(\{\mathbf{R}_I^0\}) + \frac{1}{2} \sum_{\substack{I=1 \\ J=1}}^{M,M} \sum_{\substack{I=1 \\ J=1}}^{3,3} s_{I,\mu} \Phi_{\mu\nu}(\mathbf{R}_I, \mathbf{R}_J) s_{J,\nu} \quad . \tag{7.56}$$

Inserting the displacement field for the normal modes $s_I = s_{(n,\alpha)}$ given in eq. (7.29), this can be simplified to the form

$$H^{\text{vib}} = \sum_{i=1}^{3} \sum_{\mathbf{k}} \frac{p_{(i)}^2(\mathbf{k})}{2M_{\text{ion}}} + \frac{1}{2} \sum_{i=1}^{3} \sum \mathbf{k} \omega_i^2(\mathbf{k}) \left| \mathbf{s}^{(i)}(\mathbf{k}) \right|^2 \quad , \tag{7.57}$$

where we have focused now only on the vibrational part of the ionic Hamiltonian (denoted by H^{vib}), i.e. we discard the contribution from the static minimum of the potential energy surface ($V^{\text{BO}}(\{\mathbf{R}_I^\circ\}) = 0$). With this transformation the Hamiltonian has apparently decoupled to a sum over $3M$ harmonic oscillators (compare with eq. (7.45)!), and it is thus straightforward to generalize the solution discussed in detail in the last section to this more complicated case. We define annihilation and creation operators for a phonon (i.e. normal mode) with frequency $\omega_i(\mathbf{k})$ and wave vector $\mathbf{k}$ as

$$a_i(\mathbf{k}) = \sqrt{\frac{M_{\text{ion}}\omega_i(\mathbf{k})}{2\hbar}}\, s^{(i)}(\mathbf{k}) + i \sqrt{\frac{1}{2\hbar M_{\text{ion}}\omega_i(\mathbf{k})}}\, p_{(i)}(\mathbf{k}) \tag{7.58}$$

$$a_i^\dagger(\mathbf{k}) = \sqrt{\frac{M_{\text{ion}}\omega_i(\mathbf{k})}{2\hbar}}\, s^{(i)}(\mathbf{k}) - i \sqrt{\frac{1}{2\hbar M_{\text{ion}}\omega_i(\mathbf{k})}}\, p_{(i)}(\mathbf{k}) \quad . \tag{7.59}$$

Inverting the last two expressions gives the displacement $s^{(i)}(\mathbf{k})$ and momentum $p_{(i)}(\mathbf{k})$ as a function of annihiliation and creation operators. If this is inserted into eq. (7.57) one can show (in a lengthy but straightforward calculus) that the Hamiltonian is brought to a form equivalent to eq. (7.51), i.e.

$$H^{\text{vib}} = \sum_{i=1}^{3} \sum_{\mathbf{k}} \hbar\omega_i(\mathbf{k}) \left(a_i^\dagger(\mathbf{k}) a_i(\mathbf{k}) + \frac{1}{2} \right) \quad . \tag{7.60}$$

This also implies that also the eigenvalues must have an equivalent form, namely

$$E^{\text{vib}} = \sum_{i=1}^{3} \sum_{\mathbf{k}} \hbar\omega_i(\mathbf{k}) \left(n_i(\mathbf{k}) + \frac{1}{2} \right) \quad . \tag{7.61}$$

The energy due to the lattice vibrations comes therefore from $3M$ harmonic oscillators with frequency $\omega(\mathbf{k})$. This frequency is the same as in the classic case, which is (as already remarked in the beginning of this section) why the classical analysis permitted us already to determine

the phonon band structure. In the harmonic approximation the $3M$ modes are completely independent of each other: Each such mode can be excited independently and contributes then the energy $\hbar\omega(\mathbf{k})$. While this sounds very familiar to the concept of the independent electron gas (with its energy contribution $\varepsilon_n(\mathbf{k})$ from each state $(n,\mathbf{k})$), the fundamental difference is that in the electronic system each state (or mode in the present language) can only be occupied with one electron (or two in the case of non-spin polarized systems). This results from the Pauli principle and we talk about fermionic particles. In the phonon gas, on the other hand, each mode can be excited with an arbitrary number of (indistinguishable) phonons, i.e. $n_i(\mathbf{k})$ is not restricted to the values 0 and 1. Phonons are therefore bosonic particles. The number of phonons is furthermore not constant, but is dictated by the energy of the lattice and therewith through the temperature. At $T = 0\,\mathrm{K}$ there are no phonons ($n_i(\mathbf{k}) \equiv 0$), and the lattice is "static" so to speak. Note, however, that even then the lattice energy is not zero, cf. eq. (7.61), but receives a contribution from the quantum mechanical zero-point vibrations. At increasing temperatures, more and more phonons are created, the lattice starts to vibrate and the lattice energy rises.

7.3.3 Lattice energy at finite temperatures

Having obtained the general form of the quantum mechanical lattice energy with eq. (7.61), the logical next step is to ask what this energy is at a given temperature T, i.e. we want to evaluate $E^{\mathrm{vib}}(T)$. Looking at the form of eq. (7.61), the quantity we need to evaluate in order to obtain $E^{\mathrm{vib}}(T)$, is obviously $n_i(\mathbf{k})$, i.e. the number of excited phonons in the normal mode $(\mathbf{k},\omega(\mathbf{k}))$ as a function of temperature. According to the last two sections, the energy of this mode with n phonons excited is $E_n = (n+1/2)\hbar\omega_i(\mathbf{k})$, and consequently the probability for such an excitation is proportional to $\exp(-E_n/(k_BT))$ at temperature T. Normalizing (the sum of all probabilities must be 1), we arrive at

$$P_n(T) \;=\; \frac{e^{-\frac{E_n}{k_BT}}}{\sum_l e^{-\frac{E_l}{k_BT}}} \;=\; \frac{e^{-\frac{n\hbar\omega_i(\mathbf{k})}{k_BT}}}{\sum_l e^{-\frac{l\hbar\omega_i(\mathbf{k})}{k_BT}}} \;=\; \frac{x^n}{\sum_l x^l} \quad , \tag{7.62}$$

where we have defined the short hand variable $x = \exp(-\frac{\hbar\omega_i(\mathbf{k})}{k_BT})$ in the last step. From mathematics, the value of the geometric series is known as

$$\sum_{n=0}^{\infty} x^n \;=\; \frac{1}{1-x} \quad , \tag{7.63}$$

which simplifies the probability to

$$P_n(T) \;=\; x^n(1-x) \quad . \tag{7.64}$$

With this probability the mean energy of the oscillator at temperature T becomes

$$\begin{aligned} \overline{E}_i(T,\omega(\mathbf{k})) \;=\; \sum_{n=0}^{\infty} E_n P_n(T) \;&=\; E_0 + \hbar\omega \sum_{n=1}^{\infty} n P_n(T) \\ &=\; \frac{\hbar\omega_i(\mathbf{k})}{2} + \hbar\omega_i(\mathbf{k})\,(1-x) \sum_{n=0}^{\infty} n x^n \quad . \end{aligned} \tag{7.65}$$

Differentiating eq. (7.63) on both sides, we find that

$$\sum_{n=0}^{\infty} n x^n \;=\; \frac{x}{(1-x)^2} \quad , \tag{7.66}$$

which finally leads to

$$\overline{E}_i(T,\omega(\mathbf{k})) \;=\hbar\omega_i(\mathbf{k})\left(\frac{1}{e^{\frac{\hbar\omega_i(\mathbf{k})}{k_BT}}-1}+\frac{1}{2}\right) \tag{7.67}$$

as the mean energy of this oscillating mode. Comparing with the energy levels of the mode $E_n=\hbar\omega_i(\mathbf{k})(n+1/2)$, we can identify

$$\overline{n}_i(\mathbf{k}) \;=\; \frac{1}{e^{\frac{\hbar\omega_i(\mathbf{k})}{k_BT}}-1} \tag{7.68}$$

as the mean excitation (or occupation with phonons) of this particular mode at T. This is simply the famous *Bose-Einstein statistics*, consistent with the above made remark that phonons behave as bosonic particles.
Knowing the energy of one mode at T, cf. eq. (7.67), it is easy to generalize over all modes and arrive at the total energy due to all lattice vibrations at temperature T

$$E^{\text{vib}}(T) \;=\; \sum_{i=1}^{3}\sum_{\mathbf{k}}\hbar\omega_i(\mathbf{k})\left(\frac{1}{e^{\frac{\hbar\omega_i(\mathbf{k})}{k_BT}}-1}+\frac{1}{2}\right) \quad . \tag{7.69}$$

This is still a formidable expression and we notice that the mean occupation of mode i with frequency $\omega_i(\mathbf{k})$ and wave vector $\mathbf{k}$ does not explicitly depend on $\mathbf{k}$ itself (only indirectly via the dependence of the frequency on $\mathbf{k}$). It is therefore convenient to reduce the summations over modes and wave vectors to one simple frequency integral, by introducing a *density of normal modes* (or phonon density of states) $g(\omega)d\omega$, defined so that $g(\omega)$ is the total number of modes with frequencies in the infinitesimal range between ω and $\omega+d\omega$ per volume,

$$g(\omega)d\omega \;=\; \frac{1}{(2\pi)^3}\sum_i\int d\mathbf{k}\,\delta(\omega-\omega_i(\mathbf{k}))\,. \tag{7.70}$$

This implies obviously, that

$$\int_0^\infty d\omega\, g(\omega) \;=\; 3M/V \quad , \tag{7.71}$$

i.e. the integral over all modes yields the total number of modes per volume, which is three times the number of atoms per volume, cf. section 7.2.4.
With this definition of $g(\omega)$, the total energy due to all lattice vibrations at temperature T of a solid of M atoms in a volume V takes the simple form

$$E^{\text{vib}}(T) \;=\; V\int_0^\infty d\omega\, g(\omega)\left[\frac{1}{e^{\frac{\hbar\omega}{k_BT}}-1}+\frac{1}{2}\right]\hbar\omega \quad , \tag{7.72}$$

i.e. the complete information about the specific vibrational properties of the solid is contained in the phonon density of states $g(\omega)$. Once this quantity is known, either from experiment or DFT (see the examples in Figs. 7.6 and 7.7), the contribution from the lattice vibrations can be evaluated immediately. Via thermodynamic relations, also the entropy due to the vibrations is then accessible, allowing to compute the complete contribution from the phonons to thermodynamic quantities like the free energy or Gibbs free energy.

7.3.4 Phonon specific heat

We will discuss the phonon specific heat as a representative example of how the consideration of vibrational states improves the description of those quantities that were listed as failures of the static lattice model in the beginning of this chapter. The phonon specific heat c_V measures how well the crystal can take up energy with increasing temperatures, and we had stated in the beginning of this chapter, that the absence of low energy excitations in a rigid lattice insulator would lead to a vanishingly small specific heat at lower temperatures, in clear contradiction to the experimental data. Taking lattice vibrations into account, it is obvious that they, too, may be excited with temperature. In addition, we had seen that lattice vibrational energies are in the range of thermal energies, so that the possible excitation of vibrations in the lattice should yield a strong contribution to the total specific heat of any solid. The crucial point to notice is, however, that we know from the quantum mechanical treatment, that the vibrations can not take up energy continuously (in form of gradually increasing amplitudes). Instead, only discrete excitations in form of the phonons modes are possible, and we will see that this has profound consequences on the low temperature behavior of the specific heat. That the resulting functional form of the specific heat at low temperatures agrees with the experimental data, was one of the earliest triumphs of the quantum theory of solids.

In general, the specific heat at constant volume is defined as

$$c_V(T) \;=\; \frac{1}{V}\;\left.\frac{\partial U}{\partial T}\right|_V \quad , \tag{7.73}$$

i.e. it measures (normalized per volume) the amount of energy per temperature taken up by a solid. If we want to specifically evaluate the contribution from the lattice vibrations, we arrive with the help of eq. (7.72) at the general expression

$$\begin{aligned} c_V^{\rm vib}(T) \;=\; \frac{1}{V}\;\left.\frac{\partial E^{\rm vib}}{\partial T}\right|_V \;&=\; \frac{\partial}{\partial T}\int_0^\infty d\omega\, g(\omega)\left[\frac{1}{e^{\frac{\hbar\omega}{k_BT}}-1}+\frac{1}{2}\right]\hbar\omega \\ &\simeq\; \frac{\partial}{\partial T}\int_0^\infty d\omega\, g(\omega)\left[\frac{1}{e^{\frac{\hbar\omega}{k_BT}}-1}\right]\hbar\omega \quad , \end{aligned} \tag{7.74}$$

where in the last step we have dropped the temperature-independent zero-point vibrational term.

If one plugs in the phonon densities of states from experiment or DFT, the calculated $c_V^{\rm vib}$ agree excellently with the measured specific heats of solids, proving that indeed the overwhelming contribution to this quantity comes from the lattice vibrational modes. The curves have for most elements roughly the form shown in Fig. 7.8. In particular, c_V approaches a constant value at high temperatures, while in the lowest temperature range it scales with T^3 (in metals, this scaling is in fact $\alpha T+\beta T^3$, because there is in addition the contribution from the conduction electrons, which you calculated in the first exercise). But, let us again try to see, if we can understand these generic features on the basis of the theory developed in this chapter (and not simply accept the data coming out from DFT or experiment...).

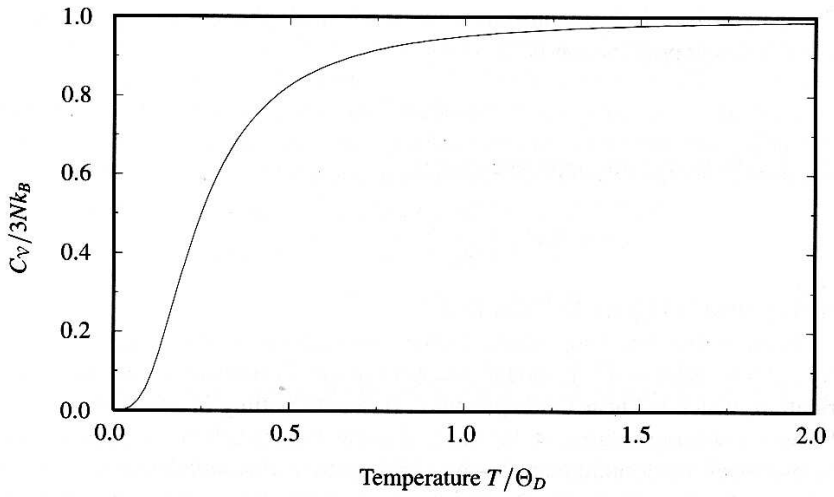

Figure 7.8: Qualitative form of the specific heat of solids as function of temperature (here normalized to a temperature Θ_D below which quantum effects become important). At high temperatures, c_V approaches the constant value predicted by Dulong-Petit, while it drops to zero at low temperatures.

High temperature limit (Dulong-Petit law)

In the high temperature limit, we have $k_BT \gg \hbar\omega$, and can therefore expand the exponential in the denominator in eq. (7.74)

$$\begin{aligned} c_V^{\text{vib}}(T\to\infty) &= \frac{\partial}{\partial T}\int_0^\infty d\omega\, g(\omega)\left[\frac{1}{e^{\frac{\hbar\omega}{k_BT}}-1}\right]\hbar\omega \\ &= \frac{\partial}{\partial T}\int_0^\infty d\omega\, g(\omega)\left[\frac{1}{(1+\frac{\hbar\omega}{k_BT}+\ldots)-1}\right]\hbar\omega \\ &= \int_0^\infty d\omega\, g(\omega)\frac{\partial}{\partial T}(k_BT) \\ &= 3k_BM/V \;=\; \text{constant} \quad , \end{aligned} \tag{7.75}$$

where in the last step we exploited eq. (7.71) for the total number of phononic states. We therefore indeed find the specific heat to become constant at high temperatures, and the absolute value of c_V^{vib} is entirely given by the density of the solid (M/V). This was long known as the *Dulong-Petit law* from classical statistical mechanics. That we recover it in this limit is simply a consequence of the fact that at such high temperatures the quantized nature of the vibrations does not show up anymore. Energy can be taken up in a quasi-continuous manner and we arrive at the classical result that each degree of freedom yields k_BT to the energy of the solid.

Intermediate temperature range (Einstein approximation)

The constant c_V^{vib} obtained in the high-temperature limit was not a surprising result, since it coincides with what we expect from classical statistical mechanics. This classical understanding can, however, not at all grasp, why the specific heat deviates at intermediate temperatures

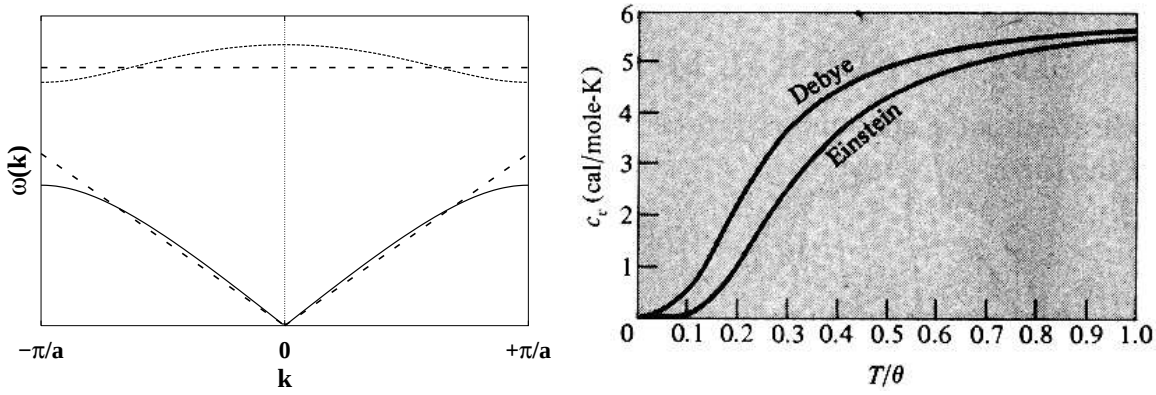

Figure 7.9: Left: Illustration of the dispersion curves behind the Einstein and Debye model (dashed curves). Einstein approximates optical branches, while Debye focuses on the acoustic branches relevant at low temperatures. Right: Specific heat curves obtained with both models.

from the constant value predicted by the Dulong-Petit law. This lowering of c_V^{vib} can only be understood on the basis of a quantum theory, namely the discrete nature of the excitation levels available for lattice vibrations. The simplest model that would go beyond a classical theory and consider this quantized nature of the oscillations is historically due to Einstein. Ignoring to zeroth order any interaction between the vibrating atoms in the solid, it is reasonable to assume that all atoms of one species vibrate with exactly one characteristic frequency (independent harmonic oscillators). This is also obvious, because without interaction, the dispersion curves of the various phonon branches become simply constant. For a mono-atomic solid, the phonon density of states breaks therefore in the *Einstein model* down to

$$g(\omega)^{\text{Einstein}} \;=\; 3(M/V)\,\delta(\omega-\omega_E) \quad , \tag{7.76}$$

where ω_E is this characteristic frequency (often called Einstein frequency), with which all atoms vibrate. Inserting this form of $g(\omega)$ into eq. (7.74) leads to

$$c_V^{\text{Einstein}}(T) \;=\; 3k_B M/V\,\left[\frac{x^2e^x}{(e^x-1)^2}\right] \quad , \tag{7.77}$$

with the short hand variable $x=\hbar\omega_E/(k_BT)$, which expresses the relation between vibrational and thermal energy. And from eq. (7.77) we see already the fundamentally important result: While in the high-temperature limit ($x \ll 1$) the term in brackets approaches unity and we recover the Dulong-Petit law, it is exactly this term that also declines for intermediate temperatures and finally drops to zero for $x \gg 1$ (i.e. $T \to 0$). The resulting specific heat curve shown in Fig. 7.9 exhibits therefore all qualitative features of the experimental data, which is a big success for such a simple model (and was a sensation hundred years ago!). To be more specific, the $c_V^{\text{Einstein}}(T)$ curve starts to deviate significantly from the Dulong-Petit value for $x \sim 1$, i.e. for temperatures $\Theta_E \sim \hbar\omega_E/k_B$. Θ_E is known as the *Einstein temperature*, and for temperatures above it, all modes can easily be excited and a classical behavior is obtained. For temperatures of the order or below Θ_E, however, the thermal energy is no longer enough to quasi-continuously excite the corresponding phonon mode, the discrete nature of the levels starts to show up, and one says that this mode starts to "freeze-out". In other words, any phonon

mode whose energy $\hbar\omega$ is much greater than $k_B T$ contributes nothing of note to the specific heat anymore, and at $T \to 0\,\mathrm{K}$, the specific heat approaches therefore zero.
Yet, precisely this limit is not obtained properly in the Einstein model. From eq. (7.77) we see that the specific heat approaches zero temperature exponentially, which is not the proper T^3 scaling known from experiment. The reason for this failure lies, of course, in the gross simplification of the phonon density of states. Approximating all modes to have the same (dispersionless) frequency is not too bad for the treatment of optical phonon branches as illustrated in Fig. 7.9. If the characteristic frequency is chosen properly in the range of the optical branches, the specific heat from this model reproduces in fact the experimental or properly computed c_V^{vib} quite well in the intermediate temperature range. This is, because at these temperatures, the specific heat is dominated by the contributions from the optical modes, whereas these modes freeze out rapidly at lower temperatures. Accordingly the model predicts a rapid exponential decline of c_V^{Einstein} to zero. While the optical branches are indeed unimportant at low temperatures, the low-energy acoustic branches may still contribute, though. And it is the contribution from the latter that gives rise to the T^3 scaling for $T \to 0\,\mathrm{K}$. Since the Einstein model does not describe acoustic dispersion well, it fails correspondingly in reproducing this limit.

Low temperature limit (Debye approximation)

To properly address the low temperature limit, we need therefore a model for the acoustic branches. For $T \to 0\,\mathrm{K}$, it will primarily be the lowest energy modes that can still be excited thermally, i.e. it is specifically the part of the acoustic branch close to the Brillouin zone center, cf. Fig. 7.9, that we should consider. In section 7.2.5 we had discussed that in this region the dispersion was linear in k, and for the corresponding very long wavelength modes the solid behaves like a continuous elastic medium. This is the conceptual idea behind the *Debye model*, which approximates $\omega_i(\mathbf{k}) = v^g k$ for all modes, with v^g the speed of sound coming out of linear elasticity theory. Note that we discuss here only a minimalistic Debye model, because even in a perfectly isotropic medium there would be at least different speeds of sound for longitudinal and transverse waves, while in real solids this gets even more differentiated. To illustrate the idea behind the *Debye model*, all of this is neglected and we use only one generic speed of sound for all phonon modes.
The important aspect about Debye is in any case not this material constant, but the linear scaling of the dispersion curves. With this linear scaling, one obtains for the phonon density of states a quadratic form

$$g(\omega)^{\mathrm{Debye}} \;=\; \frac{3}{2\pi^2 (v^g)^3}\,\omega^2\,\theta(\omega_D - \omega) \quad . \tag{7.78}$$

Since this quadratic form would be unbound for $\omega \to \infty$, a cutoff frequency ω_D (Debye frequency) is introduced, the value of which is fixed by eq. (7.71), i.e. by the requirement that the integral over $g(\omega)$ over all frequencies must yield the correct number $3(M/V)$ of the total mode density. In analogy to the Einstein model, one defines a *Debye temperature* $\Theta_D = \hbar\omega_D/k_B$, and you will show in the exercise that the specific heat in the Debye model results as

$$c_V^{\mathrm{Debye}} \;=\; 9 k_B M/V \left(\frac{T}{\Theta_D}\right)^3 \int_0^{\Theta_D/T} dx \frac{x^4 e^x}{(e^x-1)^2} \quad . \tag{7.79}$$

Similar to the Einstein model also here, the high-temperature Dulong-Petit value is obtained properly and c_V^{vib} declines to zero at lower temperatures. However, for $T \to 0\,\mathrm{K}$ the scaling is now with T^3 as immediately apparent from the above equation, i.e. as expected the Debye

model recovers therefore the correct low temperature limit. It fails on the other hand for the intermediate temperature range. As illustrated in Fig. 7.9 the Debye model deviates in this range substantially from the Einstein model, which was found to reproduce the experimental data very well. The reason is obviously that at these temperatures the optical branches get noticeably excited, the dispersion of which is badly approximated by the Debye model, cf. Fig. 7.9.

The specific heat data from a real solid can therefore be well understood from the discussion of the three ranges just discussed. At low temperatures, only the acoustic modes contribute noticeably to c_V and the Debye model provides a good description. With increasing temperatures, optical modes start to become excited, too, and the c_V curve changes gradually to the form predicted by the Einstein model. Finally, at highest temperatures all modes contribute quasi-continuously and the classical Dulong-Petit value is approached. Similar to the role of Θ_E in the Einstein model, also the Debye temperature Θ_D indicates the temperature range above which classical behavior sets in and below which modes begin to freeze-out due to the quantized nature of the lattice vibrations. Debye temperatures are normally obtained by fitting the predicted T^3 form of the specific heat to low temperature experimental data. They are tabulated for all elements and are typically of the order of a few hundred degree Kelvin, which is thus the natural temperature scale for phonons.

Note that the Debye temperature plays therefore the same role in the theory of lattice vibrations as the Fermi temperature plays in the theory of metals, separating the low-temperature region where quantum statistics must be used from the high-temperature region where classical statistical mechanics is valid. For conduction electrons, T_F is of the order of 20000 K, though, i.e. at actual temperatures we are always well below T_F in the electronic case, while for phonons both classical and quantum regimes can be encountered. This large difference between T_F and Θ_D is also responsible, why the contribution from the conduction electrons to the specific heat of metals is only noticeable at lowest temperatures. In this regime you had derived in the first exercise that c_V^{el} scales linearly with (T/T_F). On the other hand, the phonon contribution scales with $(T/\Theta_D)^3$. If we therefore equate the two, we see that the conduction electron contribution will show up only for temperatures

$$T \sim \sqrt{\frac{\Theta_D^3}{T_F}} \quad , \tag{7.80}$$

i.e. for temperatures of the order a few Kelvin.

Comparing finally the tabulated values for Θ_D with measured melting temperatures, one finds a rough correlation between the two quantities (Θ_D is about 30-50% of the melting temperature). The Debye temperature can therefore also be seen as a measure of the stiffness of the material, and reflects the critical role that lattice vibrations play also in the process of melting (which was another of the properties listed in the beginning of this chapter, where the static lattice model obviously had to fail). For the exact description of melting, however, we come to a temperature range, where the initially made assumption of small vibrations around the PES minimum and thus the harmonic approximation is certainly no longer valid. Melting is therefore one the materials properties, for which we need to go beyond the theory of lattice vibrations as we have developed it so far in this chapter.

7.4 Anharmonic effects in crystals

So far our general theory of lattice vibrations has been based on the very initial assumption that the amplitudes of the oscillations are quite small. This has led us to the so-called harmonic approximation, where higher order terms beyond the quadratic one in the Taylor expansion around the PES minimum are neglected. This approximation seems plausible, keeps the mathematics tractable and can indeed explain a wide range of materials properties. We had exemplified this in the last section for a fundamental equilibrium property like the specific heat. Similarly, we would find that lattice vibrations are central in explaining transport properties like the electric conductance. More precisely it is the scattering of the Bloch electrons as solutions of a perfect lattice at the irregularities introduced by a slightly vibrating lattice, which is important for such transport properties (which is shortly denoted as scattering at phonons in the quasi-particle picture). There are, however, also a number of materials properties, which can not be understood within a harmonic theory of lattice vibrations. The most important of these are thermal expansion and heat transport. Let's consider them in turn:

7.4.1 Thermal expansion (and melting)

In a rigorously harmonic crystal the equilibrium size would not depend on temperature. One can prove this formally (rather lengthy, see Ashcroft and Mermin), but it becomes already intuitively clear by looking at the equilibrium position in an arbitrary one-dimensional PES minimum. If we expand the Taylor series only to second order around the minimum, the harmonic potential is symmetric to both sides. Already from symmetry it is therefore clear that the average equilibrium position of a particle vibrating around this minimum must at any temperature coincide with the minimum position itself in the harmonic approximation. If the PES minimum represents the bond length (regardless of whether in a molecule or a solid), no change will therefore be observed with temperature. Only anharmonic terms, at least the cubic one, can yield an asymmetric potential and therewith a temperature dependent equilibrium position. With this understanding, it is also obvious that the dependence of elastic constants of solids on temperature and volume must result from anharmonic effects.
Let's consider in more detail the thermal expansion coefficient, α. For isotropic expansion of a cube of volume V,

$$\alpha = \frac{1}{3V}\left(\frac{\partial V}{\partial T}\right)_P \quad . \tag{7.81}$$

This can be expressed in terms of the bulk modulus, B,

$$\frac{1}{B} = \frac{1}{V}\left(\frac{\partial V}{\partial P}\right)_T \quad , \tag{7.82}$$

as

$$\alpha = \frac{1}{3B}\left(\frac{\partial P}{\partial T}\right)_V \quad . \tag{7.83}$$

Since we know that pressure, P, can be expressed as

$$P = -\left(\frac{\partial U}{\partial V}\right)_T \quad , \tag{7.84}$$

where U is the internal energy, then for α we get:

$$\alpha = \frac{1}{3B}\sum_{i,\mathbf{k}} \left(\frac{\partial \overline{\hbar\omega}_{i,k}}{\partial V}\right)_T \left(\frac{\partial \overline{n}_{i,k}}{\partial T}\right)_V \quad , \tag{7.85}$$

As 7.85 contains terms common to C_V it is common to express the thermal expansion coefficient in terms of the specific heat:

$$\alpha = \frac{\gamma C_V}{3B} \quad , \tag{7.86}$$

where γ is the Grüneisen parameter. Clearly the Grüneisen parameter is not a simple function as it embodies the variation of all normal modes in the crystal with changes of volume. Normally one defines the Grüneisen parameter for individual normal modes and it is given by

$$\gamma_{i,k} = -\frac{\partial(\ln \omega_{i,k})}{\partial(\ln V)} \quad , \tag{7.87}$$

The overall Grüneisen parameter is then determined as a weighted average in which the contribution of each mode is weighted by its contribution to C_V,

$$\gamma = \frac{\sum_{i,\mathbf{k}} \gamma_{i,k} C_V^{i,k}}{\sum_{i,\mathbf{k}} C_V^{i,k}} \quad . \tag{7.88}$$

Often γ turns out to be ~ 1 (e.g. NaCl = 1.6, KBr = 1.5), which indicates that α will exhibit a similar temperature dependence as C_V. Specifically α becomes constant at high T and at low T approaches zero as T^3.

7.4.2 Heat transport

Heat can be transported through a crystal either by the conduction electrons (metals) or by lattice vibrations (all solids). Heat in the form of a once created wave packet of lattice vibrations would travel indefinitely in a rigorously harmonic crystal, since the phonons are perfect solutions. Consequently, a harmonic solid would exhibit an infinite thermal conductance, which is analogous to the fact that a metal with a perfect rigid lattice (without defects or vibrations) would exhibit an infinite electric conductance.
For such effects, anharmonic terms beyond the quadratic one must be considered in the PES expansion. Although this is straightforward to realize, it is extremely tedious in practice. An exact treatment as in the harmonic case is then no longer possible, since the formal decoupling of the vibrational modes can no longer be achieved. Considering the effect of anharmonic terms as small perturbations, one therefore often stays within the phonon picture developed for the harmonic crystal. These phonons are now, however, no longer perfect solutions to the equations of motions, but only a first approximation. Even if one had found that the vibrations of a solids would be exactly describable by a phonon wave at a given time t, this description would become worse and worse with progressing time as the wave does not exactly fulfill the equations of motion. In the quasi-particle picture, this leads to a finite lifetime of the phonon. Phonons can therefore "decay" or scatter at each other, and we immediately see that such a concept will for example yield a finite thermal conductance.
While it is important to realize the approximate nature of the harmonic crystal model (and therefore the phonon picture), as well as understand what can be addressed within the harmonic

approach and what is due to anharmonic effects on a *conceptual level*, the actual computation of thermal expansion coefficients or thermal conductivities becomes quickly rather involved, without yielding a lot of fundamental new insight into the physics of solids. We will therefore not dwell longer on this aspect in this lecture, but refer to the literature for further reading. Corresponding treatments can e.g. be found in a complete chapter dedicated to this subject in Ashcroft and Mermin.